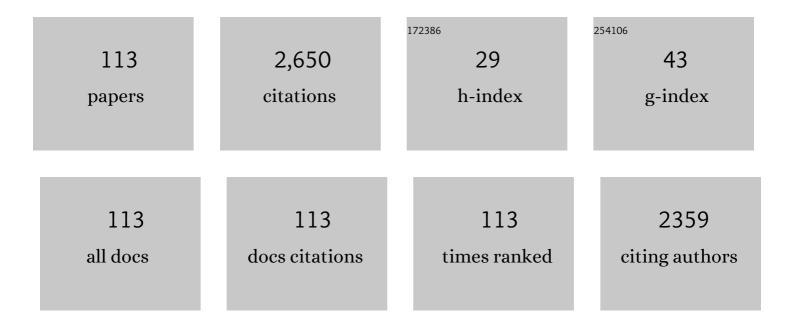
Seyed Morteza Masoudpanah

List of Publications by Year in descending order

Source: https://exaly.com/author-pdf/5243594/publications.pdf Version: 2024-02-01



#	Article	IF	CITATIONS
1	Structural characterization and magnetic properties of superparamagnetic zinc ferrite nanoparticles synthesized by the coprecipitation method. Journal of Magnetism and Magnetic Materials, 2012, 324, 3762-3765.	1.0	139
2	The microstructure, tensile, and shear deformation behavior of an AZ31 magnesium alloy after extrusion and equal channel angular pressing. Materials & Design, 2010, 31, 3512-3517.	5.1	106
3	Effects of rare-earth elements and Ca additions on the microstructure and mechanical properties of AZ31 magnesium alloy processed by ECAP. Materials Science & Engineering A: Structural Materials: Properties, Microstructure and Processing, 2009, 526, 22-30.	2.6	87
4	Synthesis of CoFe 2 O 4 powders with high surface area by solution combustion method: Effect of fuel content and cobalt precursor. Ceramics International, 2017, 43, 3797-3803.	2.3	71
5	Magnetic and microwave absorption properties of FeCo/CoFe2O4 composite powders. Journal of Alloys and Compounds, 2019, 809, 151746.	2.8	70
6	Structure and magnetic properties of La substituted ZnFe2O4 nanoparticles synthesized by sol–gel autocombustion method. Journal of Magnetism and Magnetic Materials, 2014, 370, 122-126.	1.0	69
7	Photocatalytic activity of ZnO/RGO composite synthesized by one-pot solution combustion method. Materials Research Bulletin, 2019, 115, 191-195.	2.7	60
8	Effect of fuel type on the microstructure and magnetic properties of solution combusted Fe3O4 powders. Ceramics International, 2017, 43, 7448-7453.	2.3	57
9	Effect of starting solution acidity on the characteristics of CoFe 2 O 4 powders prepared by solution combustion synthesis. Journal of Magnetism and Magnetic Materials, 2017, 424, 352-358.	1.0	56
10	Magnetic and microwave absorption properties of FeNi3/NiFe2O4 composites synthesized by solution combustion method. Journal of Alloys and Compounds, 2019, 787, 390-396.	2.8	52
11	Effects of the fuel type and fuel content on the specific surface area and magnetic properties of solution combusted CoFe 2 O 4 nanoparticles. Ceramics International, 2017, 43, 8262-8268.	2.3	51
12	Effects of pH and citric acid content on the structure and magnetic properties of MnZn ferrite nanoparticles synthesized by a sol–gel autocombustion method. Journal of Magnetism and Magnetic Materials, 2014, 357, 77-81.	1.0	48
13	Photocatalytic activity of BiFeO ₃ /ZnFe ₂ O ₄ nanocomposites under visible light irradiation. RSC Advances, 2018, 8, 6988-6995.	1.7	48
14	Mixture of fuels for solution combustion synthesis of porous Fe3O4 powders. Journal of Magnetism and Magnetic Materials, 2017, 432, 24-29.	1.0	46
15	Structural, magnetic and microwave absorption properties of SrFe12O19/Ni0.6Zn0.4Fe2O4 composites prepared by one-pot solution combustion method. Journal of Magnetism and Magnetic Materials, 2018, 466, 1-6.	1.0	46
16	Microwave-assisted solution combustion synthesis of Fe3O4 powders. Ceramics International, 2017, 43, 14756-14762.	2.3	45
17	A facial synthesis of MgFe2O4/RGO nanocomposite powders as a high performance microwave absorber. Journal of Alloys and Compounds, 2020, 834, 155166.	2.8	44
18	Synthesis and characterization of nanostructured strontium hexaferrite thin films by the sol–gel method. Journal of Magnetism and Magnetic Materials, 2012, 324, 2239-2244.	1.0	43

#	Article	IF	CITATIONS
19	Electromagnetic microwave absorption properties of high entropy spinel ferrite ((MnNiCuZn)1â^'xCoxFe2O4)/graphene nanocomposites. Journal of Materials Research and Technology, 2021, 14, 1099-1111.	2.6	42
20	Magnetic Properties of Zinc Ferrite Nanoparticles Synthesized by Coprecipitation Method. Journal of Superconductivity and Novel Magnetism, 2014, 27, 1587-1592.	0.8	41
21	Wear Behavior of Multiwalled Carbon Nanotube/AZ31 Composite Obtained by Friction Stir Processing. Tribology Transactions, 2013, 56, 827-832.	1.1	40
22	Magnetic properties of MnZn ferrite nanoparticles obtained by SHS and sol-gel autocombustion techniques. Ceramics International, 2014, 40, 6713-6718.	2.3	40
23	Solution combustion synthesis of ZnO powders using CTAB as fuel. Ceramics International, 2018, 44, 7741-7745.	2.3	39
24	The effect of post-calcination on cation distributions and magnetic properties of the coprecipitated MgFe2O4 nanoparticles. Applied Physics A: Materials Science and Processing, 2017, 123, 1.	1.1	36
25	Structural and magnetic properties of MgFe2O4 powders synthesized by solution combustion method: the effect of fuel type. Journal of Materials Research and Technology, 2020, 9, 4469-4475.	2.6	35
26	Magnetic properties of Li0.5Fe2.5O4 nanoparticles synthesized by solution combustion method. Applied Physics A: Materials Science and Processing, 2017, 123, 1.	1.1	34
27	Structural, magnetic, and gigahertz-range electromagnetic wave absorption properties of bulk Ni–Zn ferrite. Scientific Reports, 2021, 11, 9468.	1.6	34
28	PVA assisted coprecipitation synthesis and characterization of MgFe 2 O 4 nanoparticles. Ceramics International, 2017, 43, 6263-6267.	2.3	33
29	Effects of fuel contents on physicochemical properties and photocatalytic activity of CuFe2O4/reduced graphene oxide (RGO) nanocomposites synthesized by solution combustion method. Journal of Materials Research and Technology, 2020, 9, 13402-13410.	2.6	32
30	Facile synthesis of hierarchical porous Na3V2(PO4)3/C composites with high-performance Na storage properties. Journal of Power Sources, 2021, 481, 228828.	4.0	31
31	Conventional versus microwave combustion synthesis of CoFe2O4 nanoparticles. Journal of Sol-Gel Science and Technology, 2016, 79, 176-183.	1.1	30
32	Photocatalytic performances of BiFeO3 powders synthesized by solution combustion method: The role of mixed fuels. Materials Chemistry and Physics, 2019, 228, 168-174.	2.0	29
33	Solution combustion synthesis of ZnO powders using mixture of fuels in closed system. Ceramics International, 2018, 44, 12684-12690.	2.3	28
34	Photocatalytic properties of solution combustion synthesized ZnO powders using mixture of CTAB and glycine and citric acid fuels. Advanced Powder Technology, 2019, 30, 284-291.	2.0	28
35	Structural, magnetic and optical properties and photocatalytic activity of magnesium-calcium ferrite powders. Journal of Physics and Chemistry of Solids, 2021, 148, 109681.	1.9	28
36	Effects of rare earth elements and Ca additions on high temperature mechanical properties of AZ31 magnesium alloy processed by ECAP. Materials Science & Engineering A: Structural Materials: Properties, Microstructure and Processing, 2010, 527, 3685-3689.	2.6	26

#	Article	IF	CITATIONS
37	Mesoporous honeycomb-like ZnO as ultraviolet photocatalyst synthesized via solution combustion method. Materials Research Bulletin, 2019, 117, 72-77.	2.7	26
38	Effect of citric acid content on the structural and magnetic properties of SrFe12O19 thin films. Thin Solid Films, 2011, 520, 199-203.	0.8	25
39	Effect of pH value on the structural and magnetic properties of nanocrystalline strontium hexaferrite thin films. Journal of Magnetism and Magnetic Materials, 2011, 323, 2643-2647.	1.0	25
40	Solution combustion synthesis of nickel sulfide composite powders. Ceramics International, 2018, 44, 17277-17282.	2.3	24
41	A solution synthesis of Na3V2(PO4)3 cathode for sodium storage by using CTAB additive. Solid State Ionics, 2020, 347, 115269.	1.3	24
42	Different morphologies of ZnO via solution combustion synthesis: The role of fuel. Materials Research Bulletin, 2020, 125, 110784.	2.7	22
43	Hierarchical porous Fe3O4/RGO nanocomposite powders as high performance microwave absorbers. Journal of Materials Research and Technology, 2021, 13, 548-560.	2.6	22
44	The effect of the ethylene glycol to metal nitrate molar ratio on the phase evolution, morphology and magnetic properties of single phase BiFeO3 nanoparticles. Ceramics International, 2015, 41, 9642-9646.	2.3	21
45	Solution combustion synthesis of CoFe2O4 powders using mixture of CTAB and glycine fuels. Journal of Sol-Gel Science and Technology, 2018, 86, 743-750.	1.1	20
46	Thermal Decomposition Synthesis of MgFe2O4 Nanoparticles for Magnetic Hyperthermia. Journal of Superconductivity and Novel Magnetism, 2019, 32, 1347-1352.	0.8	20
47	Solution combustion synthesis of nickel sulfide/reduced graphene oxide composite powders as electrode materials for high-performance supercapacitors. Journal of Energy Storage, 2021, 39, 102637.	3.9	20
48	Enhanced electromagnetic wave absorption performance of Ni–Zn ferrite through the added structural macroporosity. Journal of Materials Research and Technology, 2022, 16, 700-714.	2.6	20
49	Fe/Sr ratio and calcination temperature effects on processing of nanostructured strontium hexaferrite thin films by a sol–gel method. Research on Chemical Intermediates, 2011, 37, 259-266.	1.3	18
50	Effects of pH value on the microstructure and magnetic properties of solution combusted Fe3O4 powders. Ceramics International, 2017, 43, 13729-13734.	2.3	18
51	Effects of ethylene glycol contents on phase formation, magnetic properties and photocatalytic activity of CuFe2O4/Cu2O/Cu nanocomposite powders synthesized by solvothermal method. Journal of Materials Research and Technology, 2021, 14, 229-241.	2.6	18
52	Microwave absorption properties of porous NiZn ferrite powders synthesized by solution combustion method: Effect of fuel contents. Journal of Alloys and Compounds, 2021, 886, 161195.	2.8	18
53	Structure and magnetic properties of nanocrystalline SrFe12O19 thin films synthesized by the Pechini method. Journal of Magnetism and Magnetic Materials, 2013, 342, 128-133.	1.0	17
54	Synthesis and Characterization of Pure Single Phase BiFeO3 Nanoparticles by the Glyoxylate Precursor Method. Journal of Superconductivity and Novel Magnetism, 2014, 27, 2795-2801.	0.8	17

SEYED MORTEZA

#	Article	IF	CITATIONS
55	Structural and optical properties of ZnAl2O4 powders synthesized by solution combustion method: Effects of mixture of fuels. Optik, 2020, 204, 164170.	1.4	17
56	Photocatalytic properties of ZnO/SnO2 nanocomposite films: role of morphology. Journal of Materials Research and Technology, 2022, 17, 2305-2312.	2.6	17
57	Magnetic properties and photocatalytic activity of ZnFe2â^'x La x O4 nanoparticles synthesized by sol–gel autocombustion method. Journal of Sol-Gel Science and Technology, 2016, 80, 487-494.	1.1	16
58	Magnetic properties of strontium hexaferrite films prepared by pulsed laser deposition. Journal of Magnetism and Magnetic Materials, 2012, 324, 2654-2658.	1.0	15
59	Magnetic and microwave absorption properties of ZnCo-substituted W-type strontium hexaferrite. Journal of Magnetism and Magnetic Materials, 2015, 382, 233-236.	1.0	15
60	Effects of Calcination Temperature on Magnetic and Microwave Absorption Properties of SrFe12O19/Ni0.6Zn0.4Fe2O4 Composites. Journal of Electronic Materials, 2020, 49, 1742-1748.	1.0	15
61	Microstructure and magnetic properties of La–Co substituted strontium hexaferrite films prepared by pulsed laser deposition. Journal of Magnetism and Magnetic Materials, 2013, 342, 134-138.	1.0	14
62	Synthesis and Characterization of Superparamagnetic Zinc Ferrite–Chitosan Composite Nanoparticles. Journal of Superconductivity and Novel Magnetism, 2015, 28, 2143-2147.	0.8	14
63	Magnetic, hyperthermic and structural properties of zn substituted CaFe2O4 powders. Applied Physics A: Materials Science and Processing, 2018, 124, 1.	1.1	14
64	Solution Combustion Synthesis of Fe3O4 Powders Using Mixture of CTAB and Citric Acid Fuels. Journal of Superconductivity and Novel Magnetism, 2019, 32, 353-360.	0.8	14
65	Preparation of strontium hexaferrite film by pulsed laser deposition with in situ heating and post annealing. Journal of Magnetism and Magnetic Materials, 2012, 324, 2894-2898.	1.0	13
66	Photocatalytic properties of ZnO powders synthesized by conventional and microwave-assisted solution combustion method. Journal of Sol-Gel Science and Technology, 2018, 86, 711-718.	1.1	13
67	Microwave-assisted solution combustion synthesis of BiFeO3 powders. Journal of Sol-Gel Science and Technology, 2018, 86, 751-759.	1.1	13
68	Solution combustion synthesis of ZnO powders using various surfactants as fuel. Journal of Sol-Gel Science and Technology, 2019, 89, 586-593.	1.1	13
69	Solution combustion synthesis of hierarchical porous LiFePO4 powders as cathode materials for lithium-ion batteries. Advanced Powder Technology, 2021, 32, 1935-1942.	2.0	13
70	Influence of metal precursor on the synthesis and magnetic properties of nanocrystalline SrFe12O19 thin films. Journal of Magnetism and Magnetic Materials, 2013, 343, 276-280.	1.0	12
71	Solution Combustion Synthesis of Ni/NiO/ZnO Nanocomposites for Photodegradation of Methylene Blue Under Ultraviolet Irradiation. Journal of Electronic Materials, 2018, 47, 2703-2709.	1.0	12
72	Correlation between shear punch and tensile measurements for an AZ31 Mg alloy processed by equal-channel angular pressing. Metallic Materials, 2021, 49, 43-50.	0.2	12

#	Article	IF	CITATIONS
73	Effect of oxygen pressure on microstructure and magnetic properties of strontium hexaferrite (SrFe12O19) film prepared by pulsed laser deposition. Journal of Magnetism and Magnetic Materials, 2012, 324, 1440-1443.	1.0	11
74	Structural, magnetic and photocatalytic characterization of Bilâ^'x La x FeO3 nanoparticles synthesized by thermal decomposition method. Bulletin of Materials Science, 2017, 40, 93-100.	0.8	11
75	CTAB-assisted solution combustion synthesis of LiFePO4 powders. Journal of Sol-Gel Science and Technology, 2019, 91, 335-341.	1.1	11
76	Effect of Reducing Agent on Solution Synthesis of Li3V2(PO4)3 Cathode Material for Lithium Ion Batteries. Molecules, 2020, 25, 3746.	1.7	11
77	Fabrication of porous Cu2S nanosheets for high performance hybrid supercapacitor. Journal of Energy Storage, 2022, 45, 103781.	3.9	11
78	Magnetic and microwave absorption properties of SrZnCoFe16O27 powders synthesized by solution combustion method. Journal of Alloys and Compounds, 2018, 739, 211-217.	2.8	10
79	Photocatalytic Activity of Nickel Sulfide Composite Powders Synthesized by Solution Combustion Method. Journal of Electronic Materials, 2020, 49, 1266-1272.	1.0	10
80	Structural, optical and photocatalytic properties of cuboid ZnO particles. Journal of Materials Research and Technology, 2021, 11, 112-120.	2.6	10
81	Effects of High-Energy Ball Milling on the Microwave Absorption Properties of Sr0.9Nd0.1Fe12O19. Journal of Superconductivity and Novel Magnetism, 2015, 28, 2715-2720.	0.8	9
82	Structural and magnetic properties of ZnFe2-xInxO4 nanoparticles synthesized by solution combustion method. Journal of Magnetism and Magnetic Materials, 2017, 442, 468-473.	1.0	9
83	L-Lysine-assisted solvothermal synthesis of hollow-like structure LiFePO4/C powders as cathode materials for Li-ion batteries. Journal of Materials Research and Technology, 2021, 15, 5405-5413.	2.6	9
84	High-performance microwave absorbers based on (CoNiCuZn)1â^'xMnxFe2O4 spinel ferrites. Journal of Alloys and Compounds, 2022, 909, 164637.	2.8	9
85	Effect of Nd3+ Substitution on the Phase Evolution and Magnetic Properties of W-Type Strontium Hexaferrite. Journal of Superconductivity and Novel Magnetism, 2016, 29, 1273-1278.	0.8	8
86	Effect of Flow Velocity and Impact Angle on Erosion–Corrosion Behavior of Chromium Carbide Coating. Journal of Tribology, 2017, 139, .	1.0	8
87	On the Interaction Between Erosion and Corrosion in Chromium Carbide Coating. Journal of Bio- and Tribo-Corrosion, 2018, 4, 1.	1.2	8
88	Magnetic and microwave absorption properties of SrZnCoFe16O27/CoFe2O4 and SrZnCoFe16O27/SrFe12O19 composite powders. Applied Physics A: Materials Science and Processing, 2019, 125, 1.	1.1	8
89	Facile synthesis of plate-like copper sulfide powder as an electrode material for high-performance supercapacitors. Journal of Materials Science: Materials in Electronics, 2020, 31, 17614-17623.	1.1	8
90	High-performance hybrid capacitors based on the FeNi3/NiFe2O4 composite powders synthesized by combustion method. Journal of Materials Research and Technology, 2022, 16, 1578-1587.	2.6	8

SEYED MORTEZA

#	Article	IF	CITATIONS
91	Synthesis and characterization of high aspect ratio NiFe2O4 nanowire. Journal of Analytical and Applied Pyrolysis, 2014, 110, 235-238.	2.6	7
92	Sol–Gel Synthesis and Characterization of SrFe12O19/TiO2 Nanocomposites. Journal of Superconductivity and Novel Magnetism, 2015, 28, 89-94.	0.8	7
93	Enhanced Photocatalytic Activity of Two-Pot-Synthesized BiFeO3–ZnFe2O4 Heterojunction Nanocomposite. Journal of Electronic Materials, 2018, 47, 2225-2229.	1.0	7
94	Facile synthesis of ZnO nanosheets as ultraviolet photocatalyst. Journal of Sol-Gel Science and Technology, 2019, 89, 594-601.	1.1	7
95	Electrochemical properties of LiMn1.5Ni0.5O4 powders synthesized by solution combustion method: Effect of CTAB as a fuel. Advanced Powder Technology, 2020, 31, 639-644.	2.0	7
96	Effect of sulfate group-containing fuels on the morphology of ZnO powders prepared by solution combustion synthesis. Journal of Materials Research and Technology, 2020, 9, 11876-11883.	2.6	7
97	Effects of flow velocity and impact angle on erosion-corrosion of an API-5 L X65 steel coated by plasma nitriding of hard chromium underlayer. Journal of Materials Research and Technology, 2020, 9, 10054-10061.	2.6	7
98	Photocatalytic performances of cobalt sulfides prepared by solution combustion synthesis using mixed fuels. Journal of Physics and Chemistry of Solids, 2021, 149, 109805.	1.9	7
99	Solution combustion synthesis of LiMn1.5Ni0.5O4 powders by a mixture of fuels. Ceramics International, 2019, 45, 22849-22853.	2.3	6
100	Salt-Assisted Solution Combustion Synthesis of Ni and Ni/NiO Powders. Journal of Superconductivity and Novel Magnetism, 2019, 32, 3321-3327.	0.8	6
101	Structure, magnetic, and microwave absorption properties of (MnNiCu)0.9â^'xCoxZn0.1Fe2O4/graphene composite powders. Journal of Alloys and Compounds, 2021, 878, 160337.	2.8	6
102	Structural, Magnetic and Photocatalytic Properties of BiFeO3 Nanoparticles. Journal of Nanostructures, 2017, 7, .	0.6	6
103	Comparison of the microstructure and magnetic properties of strontium hexaferrite films deposited on Al2O3(0001), Si(100)/Pt(111) and Si(100) substrates by pulsed laser technique. Journal of Magnetism and Magnetic Materials, 2014, 350, 81-85.	1.0	5
104	Structural and magnetic properties of Mn 0.8 Zn 0.2 Fe 2 O 4 /PVA composites. Journal of Magnetism and Magnetic Materials, 2018, 458, 80-84.	1.0	5
105	Oxalate-assisted solvothermal synthesis of octahedral LiMn1.5Ni0.5O4 particles for lithium-ion batteries. Journal of Materials Research and Technology, 2021, 13, 61-69.	2.6	5
106	Structural, microstructural, and electrochemical properties of LiFePO4 powders synthesized by mixture of fuels. Journal of Sol-Gel Science and Technology, 2021, 98, 193-201.	1.1	4
107	Solution Combustion Synthesis of BiFeO3 Powders Using CTAB as Fuel. Journal of Electronic Materials, 2019, 48, 409-415.	1.0	3
108	Combustion synthesis of porous Fe3-xZnxO4 powders for high-performance microwave absorbers. Ceramics International, 2022, 48, 14201-14209.	2.3	3

#	Article	IF	CITATIONS
109	The effects of amorphous Al2O3 underlayer on the microstructure and magnetic properties of BaFe12O19 thin films. Journal of Magnetism and Magnetic Materials, 2013, 343, 82-85.	1.0	2
110	Photocatalytic activity of solution combustion synthesized ZnO powders by using a mixture of DTAB and citric acid fuels. Journal of Physics and Chemistry of Solids, 2021, 151, 109895.	1.9	2
111	SrFeO amorphous underlayer for fabrication of c-axis perpendicularly orientated strontium hexaferrite films by pulsed laser deposition. Journal of Magnetism and Magnetic Materials, 2013, 341, 36-39.	1.0	1
112	Effect of Zn substitution on the structural and magnetic properties of densely packed Co1â^'xZnxFe2O4 Nanowires. Iranian Journal of Science and Technology, Transaction A: Science, 2018, 42, 1247-1251.	0.7	0
113	The effects of cold rolling and aging conditions on the microstructure and magnetic properties of a semi-hard Fe–Mo–Ni magnetic alloy. Journal of Materials Research and Technology, 2021, 12, 521-529.	2.6	0